http://ansinet.com/itj

ITJ

ISSN 1812-5638

INFORMATION TECHNOLOGY JOURNAL

ANSInet
Asian Network for Scientific Information
308 Lasani Town, Sargodha Road, Faisalabad - Pakistan

OPEN ACCESS Information Technology Journal

ISSN 1812-5638
DOI: 10.3923/itj.2023.1.8

Research Article
A Method for Indoor Vehicle Obstacle Avoidance by Fusion of Image and LiDAR

[1,2]Dan Li, [1,2]Jiaqiang Dong, [1,2]Kun Zhong, [1,2]Chenping Zeng and [2]Xun Cao

[1]Key Laboratory of Liangshan Agriculture Digital Transformation, Department of Sichuan Provincial Education, Xichang, 615013, China
[2]School of Information Technology, Xichang University, Xichang, 615012, China

Abstract

Background and Objective: In response to the challenges of poor mapping outcomes and susceptibility to obstacles encountered by indoor mobile vehicles relying solely on pure cameras or pure LiDAR during their movements, this paper proposes an obstacle avoidance method for indoor mobile vehicles that integrates image and LiDAR data, thus achieving obstacle avoidance for mobile vehicles. **Materials and Methods:** This method combines data from a depth camera and LiDAR, employing the Gmapping SLAM algorithm for environmental mapping, along with the A* algorithm and TEB algorithm for local path planning. In addition, this approach incorporates gesture functionality, which can be used to control the vehicle in certain special scenarios where "pseudo-obstacles" exist. The method utilizes the YOLO V3 algorithm for gesture recognition. **Results:** This paper merges the maps generated by the depth camera and LiDAR, resulting in a three-dimensional map that is more enriched and better aligned with real-world conditions. Combined with the A* algorithm and TEB algorithm, an optimal route is planned, enabling the mobile vehicles to effectively obtain obstacle information and thus achieve obstacle avoidance. Additionally, the introduced gesture recognition feature, which has been validated, also effectively controls the forward and backward movements of the mobile vehicles, facilitating obstacle avoidance. **Conclusion:** The experimental platform for the mobile vehicles, which integrates depth camera and LiDAR, built in this study has been validated for real-time obstacle avoidance through path planning in indoor environments. The introduced gesture recognition also effectively enables obstacle avoidance for the mobile vehicles.

Key words: A* algorithm, TEB algorithm, LiDAR, depth camera, obstacle avoidance

Citation: Li, D., J. Dong, K. Zhong, C. Zeng and X. Cao, 2023. A method for indoor vehicle obstacle avoidance by fusion of image and LiDAR. Inform. Technol. J., 22: 1-8.

Corresponding Author: Chenping Zeng, School of Information Technology, Xichang University, Xichang, 615012, China Tel: 18582580459

Competing Interest: The authors have declared that no competing interest exists.

Data Availability: All relevant data are within the paper and its supporting information files.

INTRODUCTION

The autonomous navigation of mobile vehicles is currently a prominent focus in the field of artificial intelligence. Path planning, a critical component of this capability, necessitates not only the utilization of algorithms to identify collision-free routes from starting points to designated destinations but also the capacity to dynamically adapt to obstacles within intricate and ever-changing environments. The efficacy of trajectory planning and obstacle avoidance performance is directly contingent upon the algorithms employed. Consequently, research efforts are concentrated on the development and refinement of path planning and obstacle avoidance algorithms.

Path planning is divided into global path planning and local path planning[1]. Global path planning algorithms are primarily responsible for finding a collision-free path from the starting point to the destination within a global map. However, they generally lack the real-time dynamic obstacle avoidance feature. Global path planning algorithms include Dijkstra's algorithm[2], A* [3], D* [4], ant colony algorithms[5], genetic algorithms[6], among others. On the other hand, local path planning algorithms are applied in situations where only a part of the environment is known or the environment is entirely unknown. These algorithms utilize information obtained from onboard sensors to provide real-time obstacle avoidance and planning capabilities. Local path planning algorithms encompass the dynamic window approach (DWA)[7], Artificial Potential Field Method[8] and time elastic band Algorithm (TEB)[9], among others. Among these algorithms, Dijkstra's algorithm lacks constraints during the search process, resulting in a large search space and reduced efficiency. In contrast, A* algorithm's heuristic search characteristic offers advantages over Dijkstra's algorithm in terms of search efficiency[10]. The DWA algorithm has a high computational complexity, making it challenging to achieve real-time dynamic obstacle avoidance. Additionally, the mobile vehicle designed in this study employs an Ackermann chassis, which does not track paths generated by DWA local path planning effectively. In contrast, the TEB algorithm not only directly supports the Ackermann chassis model but also provides time-optimal local path planning, enabling real-time and effective obstacle avoidance for local dynamic obstacles.

Achieving flawless obstacle avoidance for mobile vehicles demands the creation of precise maps. In many scenarios, single sensors are employed to reduce costs. However, these individual sensors exhibit inherent limitations that are challenging to circumvent. For instance, LiDAR, while useful, generates point cloud data with limited information content, leading to incomplete road surface perception and significantly reduced detection accuracy in adverse weather conditions[11]. Camera sensors perform well in static scenes but exhibit inadequate perception capabilities in dynamic environments. They are also susceptible to environmental factors, leading to inaccurate positioning in harsh weather conditions like strong winds or rain[12]. Ultrasonic sensors can identify transparent and reflective objects but have a limited detection range and provide subpar three-dimensional information. To address these challenges, this paper proposes an obstacle avoidance method for indoor mobile vehicles that fuses image and LiDAR data. This design combines LiDAR and depth cameras, employs the Gmapping SLAM (Simultaneous Localization and Mapping) algorithm for map construction and utilizes A* and TEB algorithms for path planning and obstacle avoidance. Additionally, this method incorporates a gesture control feature, which can be used to control the vehicle in scenarios with "pseudo-obstacles". The obstacle avoidance functionality of this design is validated through an experiment conducted on a built mobile vehicle platform. This approach not only accurately constructs environmental maps but also enables precise obstacle avoidance.

MATERIALS AND METHODS

Study area: The study was conducted at Xichang University in Xichang from April to September, 2023.

Gmapping SLAM: The Gmapping algorithm proposed by Grisetti and colleagues is an improved SLAM algorithm based on RBPF (Rao-Blackwellized Particle Filter)[13]. Its primary contribution lies in enhancing the proposal distribution and resampling selection, allowing for accurate estimation of the state of a mobile vehicle using a small number of particles and effectively addressing particle degeneracy issues. In particle filtering, the proposal distribution model typically directly employs odometric motion models. However, these odometric motion models often lead to substantial discrepancies between the proposed distribution and the true distribution. By utilizing the observation model from LiDAR data, a more concentrated distribution can be established, aligning more closely with the actual distribution[14].

The G mapping algorithm incorporates data obtained from LiDAR scans into the proposed distribution, thereby improving the proximity of the proposed distribution to the target. The enhanced proposal distribution can be represented by Eq. 1[15]:

$$p\left(x_t \middle| m_{t-1}^{(i)}, x_{t-1}^{(i)}, z_t, u_{t-1}\right) = \frac{p\left(z_t \middle| m_{t-1}^{(i)}, x_t\right) p\left(x_t \middle| x_{t-1}^{(i)}, u_{t-1}\right)}{p\left(z_t \middle| m_{t-1}^{(i)}, x_{t-1}^{(i)}, z_t, u_{t-1}\right)} \quad (1)$$

Table 1: Pseudocode for A* algorithm

```
A* Algorithm
1.  The initial node S is placed into the OPEN set.
2.  If the OPEN set is empty, then
3.      return failure
4.  else
5.      repeat
6.          Select Bestnode, from the OPEN set and move it to the CLOSE set
7.          If Bestnode is considered as the target node
8.              Success
9.          else
10.             Add Bestnode and calculate g(SUC) = g(Bestnode)+h(Bestnode, SUC)
11.             If SUC is not present in both OPEN and CLOSE sets, then
12.                 Integrate Successor into the OPEN set
13.             else
14.                 SUC=OLD, add it to the successor nodes list of Bestnode
15.                 if g(GUC)<g(OLD) then
16.                     Determine the parent node of OLD as BES and update the g(n) and f(n) values in the parent node. Mark g(OLD)
17.                 end if
18.                 Calculate h(n)
19.             end if
20.         end if
21.     Until all nodes have been traversed
22. end if
```

In Eq. 1, u_{t-1} represents the recorded self-motion information of the mobile vehicle at time t-1 during its movement, x_t signifies the estimated motion trajectory of the mobile vehicle at time t, z_t denotes the environmental information detected by the sensors at time t, x^i_{t-1} represents the state of down-sampled particles at time t-1, m^i_{t-1} represents the environmental map at time t-1.

To address the issue of particle degeneracy, the effective number of particles is calculated using Eq. 2. By comparing it with a predefined threshold, when N_{eff} is less than this threshold, the particle is considered as having a significant deviation and is subject to resampling. Otherwise, if N_{eff} exceeds the threshold, the particle is discarded. This approach reduces the frequency of resampling and mitigates the problem of particle degeneracy:

$$N_{eff} = \frac{1}{\sum\left(w^i\right)^2} \tag{2}$$

In Eq. 2, N_{eff} represents the variance of particle weights and w^i represents the weight of the i particle.

The Gmapping SLAM algorithm excels in localization and map construction due to its fusion of information from both odometry and LiDAR. It exhibits remarkable capabilities in small-scale scenarios and delivers high precision.

A* algorithms: The A* algorithm is a heuristic search algorithm and its essence lies in the design of the cost function. The mathematical model of its cost function can be represented as Eq. 3:

$$f(n) = g(n)+h(n) \tag{3}$$

In Eq. 3, g(n) represents the actual cost from the initial node to the current node n and h(n) represents the estimated cost from the current node n to the goal node. The cost function h(n) can be expressed as Eq. 4:

$$h(n) = \sqrt{\left(x_n - x_g\right)^2 + \left(y_n - y_g\right)^2} \tag{4}$$

In Eq. 4, x_n, y_n represents the coordinates of the current path node's grid center and x_g, y_g represents the coordinates of the grid center of the target node. The implementation of the A* algorithm requires the maintenance of two sets, namely, the OPEN set and the CLOSE set. The OPEN set contains all nodes that have been generated but not yet visited, while the CLOSE set contains nodes that have already been visited. Here is a pseudocode description of the implementation process of the A* algorithm as shown in Table 1[16].

TEB algorithms: The fundamental concept of the TEB algorithm is to optimize the spatial poses s_i of the mobile vehicle and the time intervals ΔT_i between consecutive poses. The spatial pose of the mobile vehicle can be denoted by

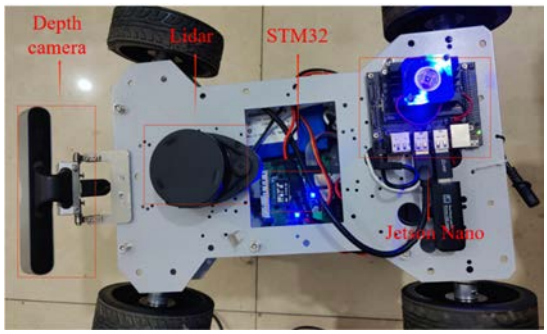

Fig. 1: Mobile vehicle experimental platform

Eq. 5, while the sequences of car poses s_i and time intervals ΔT_i are represented by Eq. 6 and 7, respectively:

$$s_i = (x_i, y_i, \beta_i)^T \quad (5)$$

$$S = s_i \ (i = 0,1\ldots n, n \in N) \quad (6)$$

$$\tau = \Delta T_i \ (i = 0, 1...n\text{-}1, n \in N) \quad (7)$$

In Eq. 5, x_i, y_i represents the two-dimensional coordinates of the mobile vehicle in the world coordinate system[17] and β_i represents the pose of the mobile vehicle. The TEB trajectory expression that includes the sequence of mobile vehicle poses and time intervals is given by Eq. 8:

$$B: = (S, \tau) \quad (8)$$

On this basis, a weighted multi-objective optimization is performed by considering various dynamic constraints such as path optimality, avoidance of obstacles, car velocity and acceleration. This optimization is subsequently solved using the open-source G2O (General Graph Optimization, G2O) library to obtain a locally optimal trajectory B* that satisfies the specified conditions[17]. The functional expression for this process is provided in Eq. 9:

$$\begin{cases} f(B) = \sum_k \gamma_k f_k(B) \\ B^* = \text{argmin}_B f(B) \end{cases} \quad (9)$$

In Eq. 9, f(B) represents the total objective function, $f_k(B)$ represents the objective functions associated with different constraints, γ_k represents the weights assigned to each term and B* represents the optimal TEB trajectory.

Fusion mapping with depth camera and LiDAR: The experimental platform for the indoor mobile vehicle established in this study was depicted in Fig. 1. This vehicle is equipped with domestic sensors, including the RPLIDAR A1 LiDAR, the LeTMC-520 depth camera and an IMU odometer. The upper-level computer system is powered by a 9th-generation Core i7 CPU, GTX1660TI GPU and boasts 512GB of memory. The lower-level control unit employs an STM32F407 driver board and is controlled by a Jetson Nano overseeing the upper-level system. The vehicle chassis adheres to an Ackermann structure. Operating on the Linux operating system, the upper-level computer utilizes the Robot Operating System (ROS), with programming conducted in Python and C++. The experiments were conducted under enclosed indoor conditions, validating the system's performance.

The indoor conditions refer to the electronic information laboratory at the school, which is primarily used for the construction and debugging of the mobile vehicle platform. The obstacle avoidance tests for the mobile vehicle are conducted in a more complex home environment.

RESULTS AND DISCUSSION

Research on obstacle avoidance for mobile vehicles has been extensive, with the majority of recent studies adopting multisensory fusion techniques to attain accurate maps for the implementation of mobile vehicles obstacle avoidance[2,17-23]. The approaches adopted in these studies generally follow a common technical route: Initially, an algorithm is employed to construct an environmental map; subsequently, another algorithm is utilized for path planning to achieve obstacle avoidance. Finally, an experimental platform is established for testing, aiming to validate the effectiveness of obstacle avoidance and to assess its superior performance compared to single-sensor methods. However, none of these prior works presents a specific metric for quantifying the effectiveness of obstacle avoidance. Consequently, this paper cannot be directly compared to the outcomes of the previous literature. The methodology employed in this paper follows a similar technical route to previous works, with the distinctive incorporation of gesture recognition capabilities, building upon existing research. This augmentation enables effective obstacle avoidance, even in the presence of "pseudo-obstacles".

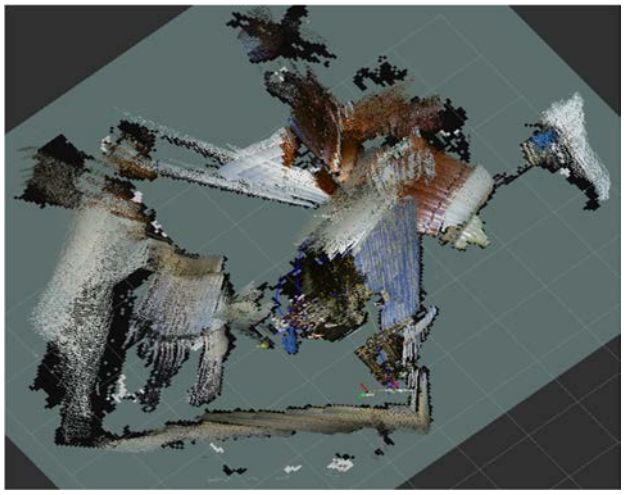

Fig. 2: Mapping using only the depth camera

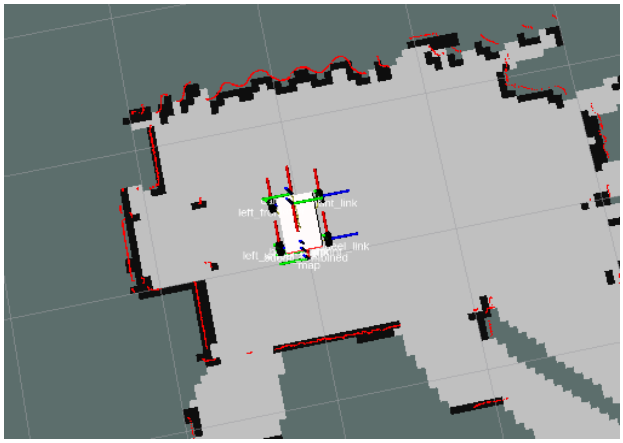

Fig. 3: Mapping using only the LiDAR

Mapping and obstacle avoidance for the mobile vehicle: When using only the depth camera for mapping, the depth camera captures depth images of the real environment, allowing the creation of a three-dimensional local environment map. The result of pure camera-based mapping, as shown in Fig. 2, exhibits poor mapping quality with significant information loss and overlapping data. The image shows numerous folds and distortions, primarily due to the depth camera's limited accuracy in providing distance information, particularly when the vehicle speed exacerbates image distortion and overlap. Alternatively, when using only the LiDAR for mapping, the LiDAR collects information from the real environment and generates a two-dimensional point cloud contour of the indoor environment. Simultaneously, the motor encoders record the number of rotations of the mobile vehicle driving wheels, providing odometry data. This data is then input into the Gmapping algorithm, resulting in the mapped output shown in Fig. 3. Figure 3 revealed inaccuracies in laser distance measurements due to the presence of objects with weak laser reflectivity in real-world conditions, such as curtains, vegetation, wire fences and various flexible materials. Therefore, this paper combines the maps generated by the depth camera and LiDAR, resulting in a three-dimensional fusion mapping as shown in Fig. 4. In this representation, the black edges represent information provided by the LiDAR, while all other information is obtained from the depth camera. It is evident that the fusion mapping provides richer and more realistic information. Consequently, using such a three-dimensional map, the vehicle can acquire obstacle information and, in conjunction with A* and TEB algorithms, plan an optimal route, thereby achieving obstacle avoidance.

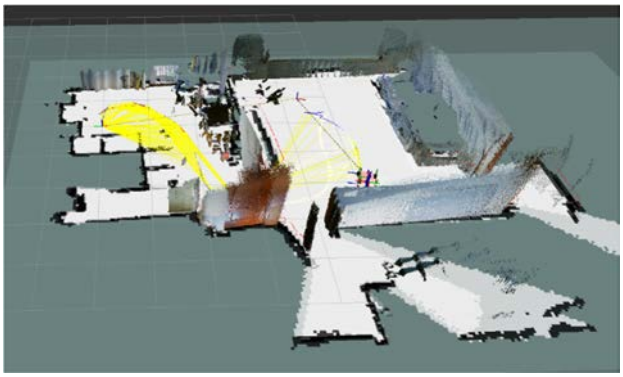

Fig. 4: Three-dimensional fusion mapping

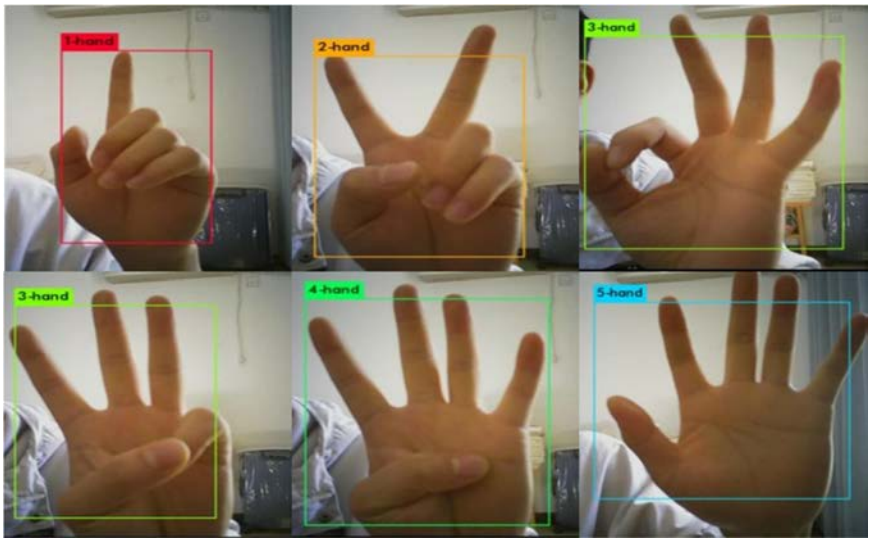

Fig. 5: Gesture recognition

Gesture recognition: Gesture recognition is equally important in obstacle avoidance. It can be used to control the mobile vehicle when encountering "pseudo-obstacles." These pseudo-obstacles might include small objects with low height and volume on the road, such as stones or bricks, as well as unexpected intrusions like birds, paper scraps, or leaves. These are referred to as "pseudo-obstacles."

In this paper, the YOLO V3 algorithm is initially employed for gesture recognition. Subsequently, recognized gestures are used to implement basic motion control for the mobile vehicle. Currently, only gestures 2 and 3 are configured with functionalities, while other gestures have not been assigned specific functions, leaving room for future enhancements. The results of gesture recognition were shown in Fig. 5 and tests conducted on gestures 2 and 3, which trigger predefined actions based on gestures, were presented in Fig. 6.

In Fig. 6a, when performing Gesture 2 in front of the camera, the mobile vehicle rear wheels start to rotate clockwise, accelerating for 2 sec before stabilizing at a constant speed. If the vehicle is placed on the ground, it will accelerate in reverse and then maintain a constant speed in reverse motion. On the other hand, when performing Gesture 3 in front of the camera, the mobile vehicle rear wheels start to rotate counterclockwise, accelerating for 2 sec before stabilizing at a constant speed (Fig. 6b). If the vehicle is placed on the ground, it will accelerate forward and then maintain a constant speed in forward motion. This validates the capability to control the forward or backward movement of the mobile vehicle through gestures, achieving obstacle avoidance.

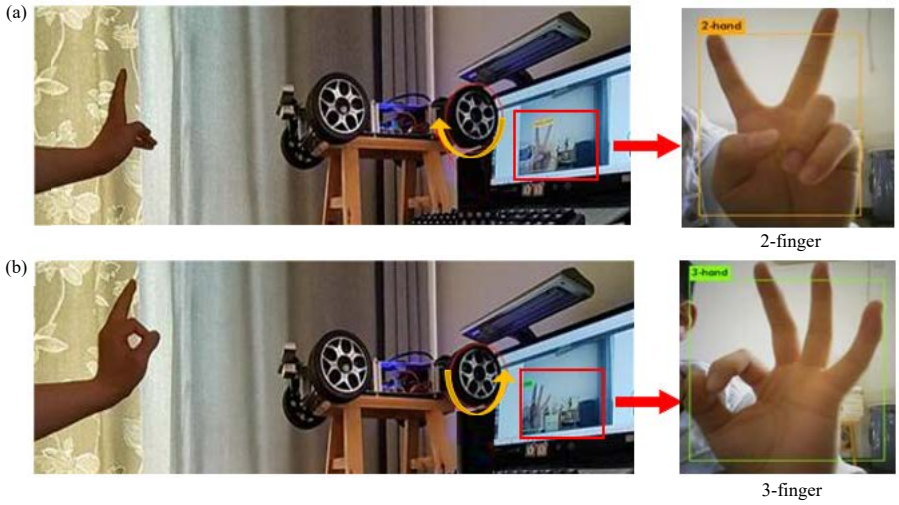

Fig. 6(a-b): Gesture recognition test results for mobile vehicle, (a) When Gesture 2 is made, the rear wheels of the mobile vehicle will rotate clockwise, indicating a backward motion and (b) When Gesture 3 is made, the rear wheels of the mobile vehicle will rotate counterclockwise, indicating a forward motion

However, there are some limitations:

- The logic connections between the main control and subordinate modules are complex, requiring multiple communication lines. The lack of standardized interfaces has led to a messy tangle of wires, even if they are hidden beneath the vehicle base. This makes troubleshooting difficult
- Subordinate STM32 module needs to handle high voltages and is susceptible to wear and tear. It cannot be integrated into a single development board with the main control, making it challenging to establish a perfect communication solution

CONCLUSION

This study has developed a mobile vehicle platform that integrates a depth camera with a LiDAR sensor. It employs the Gmapping SLAM algorithm for environment mapping, uses the A* algorithm for global path planning and utilizes the TEB algorithm for local path planning to achieve real-time obstacle avoidance. Additionally, it has implemented obstacle avoidance through gesture recognition. Future research will aim to address these issues. Efforts will be made to unify the connections between the main control, subordinate modules and various interfaces, ensuring both aesthetics and ease of troubleshooting by providing designated wiring locations on the vehicle body. Additionally, the goal is to integrate the main control and subordinate modules onto a single board, improving communication efficiency.

SIGNIFICANCE STATEMENT

With the increasing frequency of traffic accidents, the development of autonomous driving technology, which relies on computer control instead of driver operation, serves as an important means to mitigate human-operated risks and effectively address this issue. Therefore, this article explores autonomous driving technology by researching algorithms related to mobile vehicles and obstacle avoidance.

ACKNOWLEDGMENTS

This work was supported by the Liangshan Intelligent Agriculture Sensing Technology Research and Development Laboratory (grant number 015/117236000), Xichang University Doctoral Research Project (grant number YBZ202107) and Optical Fiber Sensing Technology for Smart Agriculture Research Team (grant number 015/117279029).

REFERENCES

1. Tosun, D.C. and Y. Işık, 2023. A ROS-based hybrid algorithm for the UAV path planning problem. Aircr. Eng. Aerosp. Technol., 95: 784-798.
2. Zhu, D.D. and J.Q. Sun, 2021. A new algorithm based on Dijkstra for vehicle path planning considering intersection attribute. IEEE Access, 9: 19761-19775.

3. Wang, R., Z. Lu, Y. Jin and C. Liang, 2022. Application of A* algorithm in intelligent vehicle path planning. Math. Models Eng., 8: 82-90.
4. Karur, K., N. Sharma, C. Dharmatti and J.E. Siegel, 2021. A survey of path planning algorithms for mobile robots. Vehicles, 3: 448-468.
5. Miao, C., G. Chen, C. Yan and Y. Wu, 2021. Path planning optimization of indoor mobile robot based on adaptive ant colony algorithm. Comput. Ind. Eng., Vol. 156. 10.1016/j.cie.2021.107230.
6. Pan, Y., Y. Yang and W. Li, 2021. A deep learning trained by genetic algorithm to improve the efficiency of path planning for data collection with multi-UAV. IEEE Access, 9: 7994-8005.
7. Wang, H., X. Ma and L. Zhu, 2022. Obstacle avoidance path planning of mobile robot based on improved DWA. J. Phys.: Conf. Ser., Vol. 2383. 10.1088/1742-6596/2383/1/012098.
8. Duhé, J.F., S. Victor and P. Melchior, 2021. Contributions on artificial potential field method for effective obstacle avoidance. Fract. Calc. Appl. Anal., 24: 421-446.
9. Sun, J., Z. Sun, P. Wei, B. Liu, Y. Wang, T. Zhang and C. Yan, 2023. Path planning algorithm for a wheel-legged robot based on the Theta* and timed elastic band algorithms. Symmetry, Vol. 15. 10.3390/sym15051091.
10. Foead, D., A. Ghifari, M.B. Kusuma, N. Hanafiah and E. Gunawan, 2021. A systematic literature review of A* pathfinding. Procedia Comput. Sci., 179: 507-514.
11. Heinzler, R., F. Piewak, P. Schindler and W. Stork, 2020. CNN-based lidar point cloud de-noising in adverse weather. IEEE Rob. Autom. Lett., 5: 2514-2521.
12. Liu, Z., Y. Cai, H. Wang, L. Chen, H. Gao, Y. Jia and Y. Li, 2022. Robust target recognition and tracking of self-driving cars with radar and camera information fusion under severe weather conditions. IEEE Trans. Intell. Transp. Syst., 23: 6640-6653.
13. Kegeleirs, M., G. Grisetti and M. Birattari, 2021. Swarm SLAM: Challenges and perspectives. Front. Robot. AI, Vol. 8. 10.3389/frobt.2021.618268.
14. Grisetti, G., C. Stachniss and W. Burgard, 2007. Improved techniques for grid mapping with rao-blackwellized particle filters. IEEE Trans. Rob., 23: 34-46.
15. Tian, C., H. Liu, Z. Liu, H. Li and Y. Wang, 2023. Research on multi-sensor fusion SLAM algorithm based on improved gmapping. IEEE Access, 11: 13690-13703.
16. Tang, G., C. Tang, C. Claramunt, X. Hu and P. Zhou, 2021. Geometric a-star algorithm: An improved a-star algorithm for AGV path planning in a port environment. IEEE Access, 9: 59196-59210.
17. Wu, J., X. Ma, T. Peng and H. Wang, 2021. An improved timed elastic band (TEB) algorithm of autonomous ground vehicle (AGV) in complex environment. Sensors, Vol. 21. 10.3390/s21248312.
18. Li, S., Z. Li, Z. Yu, B. Zhang and N. Zhang, 2019. Dynamic trajectory planning and tracking for autonomous vehicle with obstacle avoidance based on model predictive control. IEEE Access, 7: 132074-132086.
19. Lv, J., C. Qu, S. Du, X. Zhao, P. Yin, N. Zhao and S. Qu, 2021. Research on obstacle avoidance algorithm for unmanned ground vehicle based on multi-sensor information fusion. Math. Biosci. Eng., 18: 1022-1039.
20. Xu, R., 2019. Path planning of mobile robot based on multi-sensor information fusion. EURASIP J. Wireless Commun. Networking, Vol. 2019. 10.1186/s13638-019-1352-1.
21. Wang, Z., Y. Wu and Q. Niu, 2019. Multi-sensor fusion in automated driving: A survey. IEEE Access, 8: 2847-2868.
22. Zhang, X., T. Zhu, L. Du, Y. Hu and H. Liu, 2022. Local path planning of autonomous vehicle based on an improved heuristic Bi-RRT algorithm in dynamic obstacle avoidance environment. Sensors, Vol. 22. 10.3390/s22207968.
23. Wu, H.,Y. Zhang, L. Huang, J. Zhang, Z. Luan, W. Zhao and F. Chen, 2023. Research on vehicle obstacle avoidance path planning based on APF-PSO. Proc. Inst. Mech. Eng. Part D: J. Automob. Eng., 237: 1391-1405.